A Method to Control Unstable Hopf Bifurcation in Power Systems

Sang-Ho Lee* and Jong-Keun Park**

Abstract - The model of a power system with load dynamics is studied by investigating qualitative changes in its behavior as the reactive power demand at a load bus is increased. The load is created using induction motors parallel with the constant power and constant impedance load. As the load increases, the system experiences various bifurcations such as subcritical and supercritical Hopf, period-doubling and saddle-node bifurcation. The latter may lead the system to voltage collapse. A nonlinear controller is used to control the subcritical Hopf bifurcation and hence mitigate voltage collapse. It is applied to the KEPCO (Korean Electric Power Company) system to demonstrate its validity.

Keywords: subcritical and supercritical Hopf bifurcation, voltage collapse, nonlinear controller

1. Introduction

Stability factors experienced by power systems have become increasingly important since the introduction of the complex load to the power systems. A power system generally expresses highly nonlinear dynamic equations including several system parameters. The response of the system can be to undergo various bifurcations such as Hopf, period-doubling, or saddle-node bifurcation, any of which can lead the power system to voltage collapse. Voltage collapse is the process by which voltage instability results in a very low profile situation in a certain portion of the system and, ultimately induces the general blackout of a segment or of the totality of the network. The collapse may be followed by the loss of load or the tripping of lines, or even worse, complete shutdown of the affected area.

To enhance the unstable situation, many techniques are presently in use to mitigate voltage collapse. These techniques include: a) series capacitor banks, b) static var compensators (SVC), and c) operating uneconomic generators to change power flows or provide voltage support during emergencies. Some investigators have linked voltage collapse to static bifurcations, in particular, saddle-node bifurcations. Kwanty et al. presented an analysis of static stability in power systems based on a model consisting of the classical swing-equation characterization for generators and a constant admittance [1]. Abed & Varajya were the first to suggest a possible role for dynamic bifurcations in voltage collapse phenomena [2]. Later Abed et al. [3], Dobson & Chiang [4], Ajjarapu and Lee [5], Venkatasubramanian et al. [6] and Nayfeh et al.[7] investigated oscillatory behaviors of power systems and their implication on voltage collapse.

Over the past decade, there has been an interest in the interplay between bifurcation and control theories as well as in applications of bifurcation theory in the design of controllers for nonlinear systems exhibiting bifurcations. Abed et al. [3] investigated the mitigation of Hopf bifurcations and chaos by using bifurcation control. They proposed controllers of the form $y = K\omega^n$, where n=1,3, ω is the frequency, and K>0 is the gain [7]. They use the techniques of perturbation theories [10] and nonlinear feedback control [9].

In general, the power system model can be represented by a system of nonlinear algebraic and ordinary differential equations. The loads can be classified into static loads (e.g., constant impedance, constant current or constant power) and dynamic loads (e.g. induction motors). In all of the aforementioned studies, the loads have been modeled in induction motors, capacitors, and constant PQ loads. According to past experiences, the power transfer capability of a long transmission line for any type of compensation scheme is the highest for a constant impedance load and the lowest for a constant power load [8]. In the present work, we consider a model in which the load is represented by an induction motor, a capacitor, and a combination of constant power and constant impedance PQ loads. Then, voltage stability is studied by investigating the bifurcation of static and dynamic solutions.

2. Power System Model

We consider after Dobson & Chiang the power system shown in Fig.1 [4]. It consists of two generators feeding a

* Korea Electrotechnology Research Institute, Korea (lee-sangho@keri.re.kr)
** School. of Electrical Engineering, Seoul National University, Korea (pakrjk@snu.ac.kr)
Received April 18, 2003 ; Accepted October 14, 2003

load, which is represented by an induction motor in parallel with a capacitor and a PQ load. One generator is an infinite bus and the other generator has a constant voltage magnitude E_m.

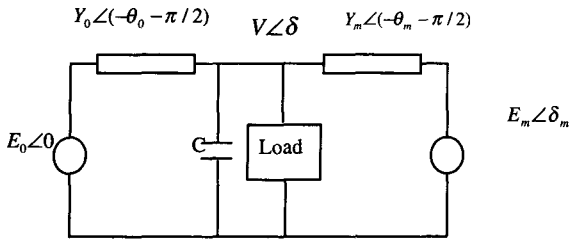

Fig. 1 Power system model (3 bus system)

The equations that govern the power system model are:

$$\dot{\delta}_m = \omega \tag{1}$$

$$M\dot{\omega} = -d_m\omega + P_m + E_m Y_m V \sin(\delta - \delta_m - \theta_m) + E_m^2 Y_m \sin\theta_m \tag{2}$$

$$K_{qw}\dot{\delta} = E_0 Y_0 V\cos(\delta+\theta_0) + E_m Y_m V\cos(\delta-\delta_m+\theta_m) - [K_{qv2} + q_3 Q_1 + Y_0\cos\theta_0 + Y_m\cos\theta_m]V^2 - (K_{qv} + q_2 Q_1)V - (Q_0 + q_1 Q_1) \tag{3}$$

$$TK_{qw}K_{pv}\dot{V} = -\sqrt{K_{qw}^2 + K_{pw}^2}[-E_0 Y_0 V\cos(\delta + \theta_0 - \eta) + E_m Y_m V\cos(\delta - \delta_m + \theta_m - \eta)] + [K_{pw}K_{qv2} + \sqrt{K_{qw}^2 + K_{pw}^2}[Y_0\cos(\theta_0 - \eta) + Y_m\cos(\theta_m - \eta)] - K_{qw}p_3P_1 + K_{pw}q_3Q_1]V^2 + [K_{pw}K_{qv} - K_{qw}K_{pv} - K_{qw}p_2P_1 + K_{pw}q_2Q_1]V - K_{qw}(P_0 + p_1P_1) + K_{pw}(Q_0 + q_1Q_1) \tag{4}$$

where $\eta = \tan^{-1}(K_{qw} + K_{pw})$

We have four state variables, namely, $\delta_m, \omega, V, \delta$ and many control parameters. These equations admit equilibrium as well as dynamic solutions. Equilibrium solutions are discussed in Sec. 3, whereas dynamic solutions are discussed in Sec. 4.

In most aforementioned studies [3, 4], the PQ load has been represented as a constant power, that is p_2, p_3, q_2, and q_3 are taken to be zero. In this paper, to realize the influence of constant impedance load and constant power load, we set $q_1 = q_3 = 1$.

Q_1 is used as the control parameter. We use the same parameter value in [4].

$K_{pw} = 0.4, K_{pv} = 0.3, K_{qw} = -0.03, K_{qv} = -2.8,$
$K_{qv2} = 2.1, T = 8.5, P_0 = 0.6, Q_0 = 1.3, E_0 = 1.0,$
$C = 12.0, Y_0 = 20.0, \theta_0 = -5.0, Y_m = 5.0, \theta_m = -5.0,$
$E_m = 1.0, P_m = 1.0, d_m = 0.05, M = 0.3$

All values are in per unit except for angles, which are in degrees.

3. Approximated Equilibrium Solutions And Their Bifurcations

The equilibrium solutions of (1)~(4) correspond to

$$\dot{\delta} = 0 \quad (5) \qquad \dot{\omega} = 0 \quad (6)$$

$$\dot{\delta}_m = 0 \quad (7) \qquad \dot{V} = 0. \quad (8)$$

It is not easy to estimate the equilibrium solution for these equations analytically. However, under the assumption of $\delta_m \approx \delta \approx 0$, we can obtain the approximated solution for V and declare the static limit of the system easily from (8). Since (8) is quadratic in V ($aV^2 + bV + c = 0$), the static limit can be simply determined by its discriminant D ($b^2 - 4ac$). The discriminant is plotted in Fig. 2. We also plot the approximated equilibrium solution of V and the discriminant D in Fig. 3.

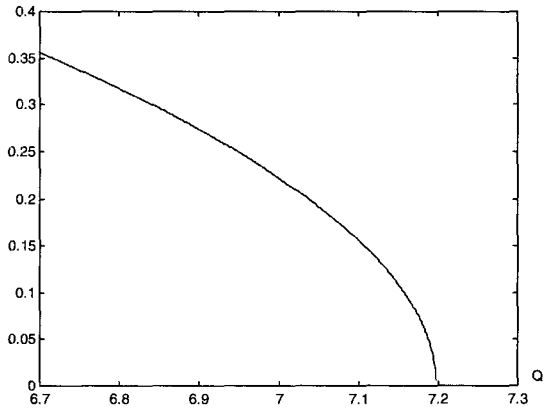

Fig. 2 Discriminant of approximated equation of (8)

The discriminant has a form similar to the voltage profile, so we can use this as an index for static voltage limit. That is, if the value of discriminant reaches zero, it

signifies that the voltage is approaching the saddle-node bifurcation point. But under this assumption, no Hopf bifurcation can be viewed since we ignore the sine function of angles. It is verified that this assumption is quite acceptable through the numerical simulation in the next section.

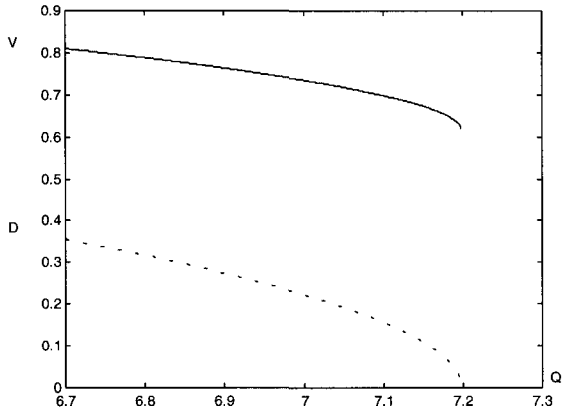

Fig. 3 Approximated equilibrium solution and discriminant

4. Dynamic Solutions

A representative bifurcation diagram for the case of a constant and quadratic PQ load (i.e. a combination of constant power and constant impedance load) is shown in Fig. 4. Throughout all simulations, the dynamic simulation package PSS/E has been used.

There are two Hopf bifurcations HB1 and HB2 at Q_1=6.9739 and 7.19403, respectively, and a saddle-node bifurcation at Q_1=7.19505.

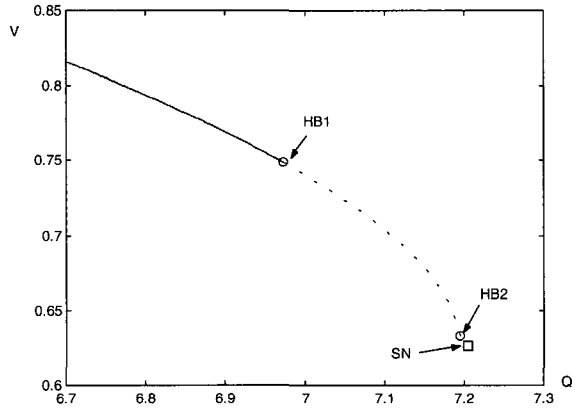

Fig. 4 Bifurcation diagram for the uncontrolled system

The limit value and solutions are nearly identical to those in Fig. 2, so the assumption of $\delta_m \approx \delta \approx 0$ in section 3 is reasonable.

The solid and dashed lines are used to depict the loci of stable and unstable equilibrium states, respectively. HB1 and HB2 represent the subcritical and supercritical Hopf bifurcation point, respectively. Near the Hopf bifurcation points HB1 and HB2, (1)~(4) possess small limit cycle solutions.

Between HB1 and HB2, the stable limit cycles undergo a sequence of period-doubling bifurcations, culminating in chaos. The chaotic attractors in turn suffer crises-type bifurcations, leading to voltage collapse. One example for the unstable behavior is depicted in Fig. 5.

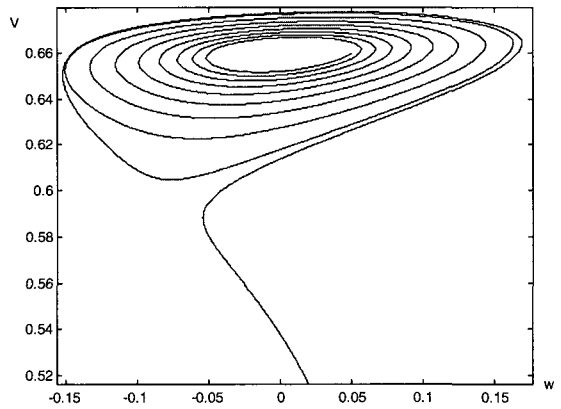

Fig. 5 A two-dimensional projection of the phase portrait onto the V-ω plane (Q_1=6.98: just after the crisis)

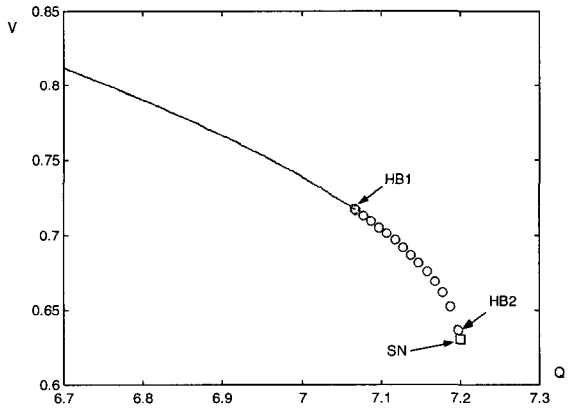

Fig. 6 Bifurcation diagram for the controlled system

Starting with a value of Q_1 slightly less than that corresponding to the saddle-node bifurcation value of Q_1=7.19505 and slowly decreasing Q_1, we find that V is constant and stable. As Q_1 decreases below the supercritical Hopf bifurcation HB2 at Q_1=7.19403, a small and stable limit cycle begins to take shape. As Q_1 decreases further, the limit cycle grows, deforms, and then endures a sequence of period-doubling bifurcations, leading to chaos.

5. Control Of Subcritical Hopf Bifurcaition

To control the subcritical Hopf bifurcation and hence the chaos and voltage collapse, we added a nonlinear feedback controller that transforms the Hopf bifurcation from a subcritical state into a supercritical one. The nonlinear load dynamics are known as the main cause of voltage instability. Therefore, the controller in the load bus has a superior effect on voltage instability. We added the nonlinear controller to eq. (4) of the form $K_1V - K_3V^3$. ($K_1 = 0.1, K_3 = 0.2$) The cubic term plays the role of a stabilizing factor if it has a negative coefficient. The opposite sign of the linear term is added to prevent the decrease of voltage caused by a minus term (cubic term). The linear term is a destabilizing term, so it must have a relatively insignificant value.

The subcritical Hopf bifurcation HB1 has been transformed into a supercritical Hopf bifurcation, the unstable limit cycles have been eliminated, and the amplitudes of the stable limit cycles born as a result of the Hopf bifurcation are small. Consequently, voltage collapse has been delayed to the saddle-node bifurcation point.

In Fig. 6, stable oscillatory states are denoted by circles and the saddle-node bifurcation point is denoted by a square.

A case of stable limit cycle is depicted in Fig. 7. In this case, any small disturbance will trigger the systems stable limit cycle.

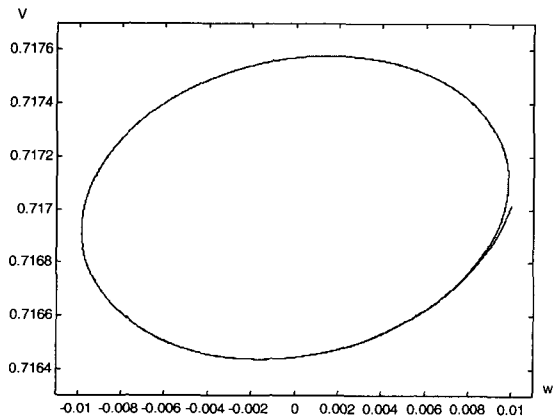

Fig. 7 A two-dimensional projection of the phase portrait onto the V-ω plane: the case of stable limit cycle

6. Application To Kepco System

To verify the validity of this controller, we applied it to the KEPCO system composed of 215 machines and 803 buses. Fig. 8 shows the bifurcation diagram for bus 1445. The 'x's in Fig. 8 represent the unstable oscillatory solutions. The small square is the saddle-node bifurcation point.

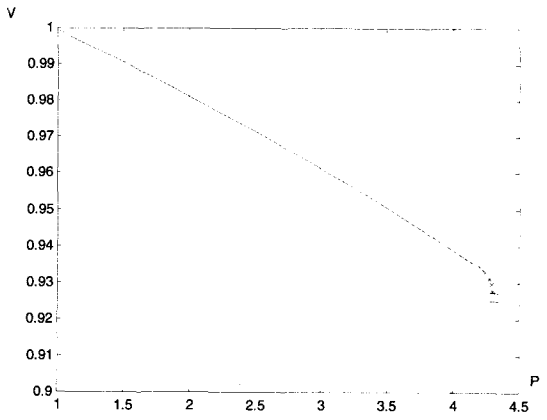

Fig. 8 Bifurcation diagram for the uncontrolled KEPCO system

A time sequence of voltage in some buses (#5645, #23371) is given in Fig. 9. The magnitude of voltage increases with time.

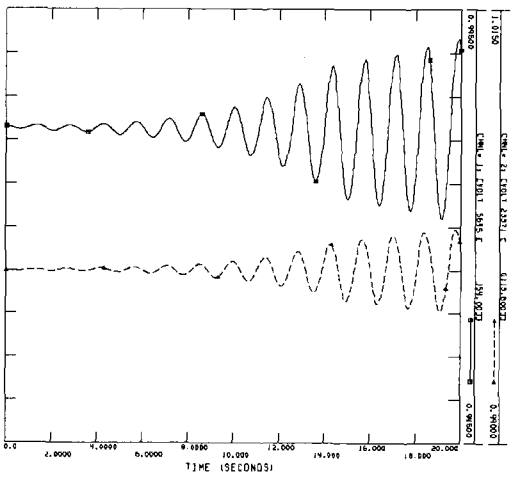

Fig. 9 Voltage profiles around the unstable Hopf bifurcation

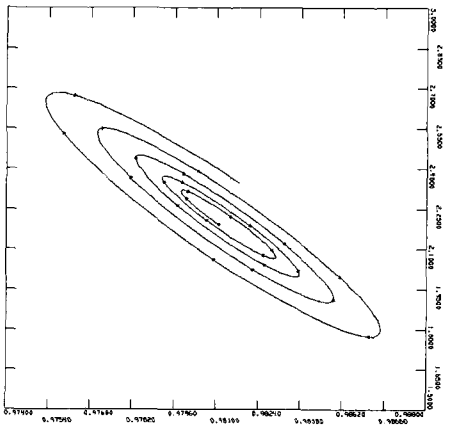

Fig. 10 Unstable limit cycle

To improve this situation, the nonlinear controller of $K_1V - K_3V^3$ is added to this bus, so that the unstable oscillatory solutions are transformed into stable ones.

One of its examples is depicted in Fig. 9 and Fig. 10. Fig. 9 is representative of the uncontrolled system and Fig. 10 is the supercritical Hopf bifurcation trajectory with the nonlinear controller. The x-axis is the voltage and the y-axis is the var output of the generator #25151 in both figures.

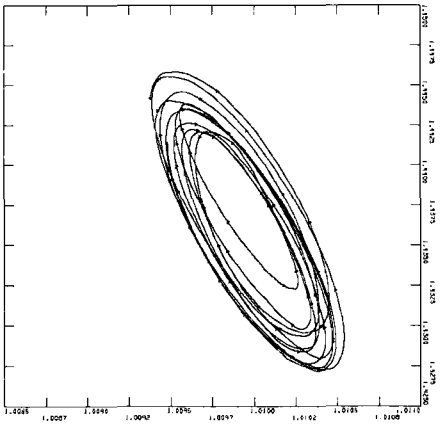

Fig. 11. Stable limit cycle

5. Conclusion

We have considered the model power system with two generators feeding a load represented by an induction motor in parallel with a capacitor and a PQ load.

Under some degree of assumption, a static stability index can be derived and an approximated equilibrium solution can be acquired easily. This has been verified through numerical simulation.

Dynamic solutions indicate that the system can be unstable through subcritical Hopf bifurcation, so a nonlinear controller is added in the load bus to convert unstable Hopf bifurcation into stable Hopf bifurcation. This can mitigate voltage collapse until the point of saddle-node bifurcation.

This scheme has been applied to the KEPCO system, so that the unstable oscillatory phenomena can be suppressed.

References

[1] Kwatny, H.G., Pasrija, A.K. and Bahar, L.Y., "Static Bifurcation in Electric Power Network: Loss of Steday-State Stability and Voltage Collapse", *IEEE Trans. on Circuits and Systems*, 1986, pp.981-991

[2] Abed, E.H. and Varaiya, "Nonlinear Oscillations in Power Systems", *International Journal of Electric Power and Energy System 6*, 1984, pp.37-43

[3] Abed, E.H., Wang, H.O., and Chen, "Stabilization of Period Doubling Bifurcation and Implications for Control of Chaos", *IEEE Proc. of the 31th IEEE Conf. on Decision and Control*, 1992, pp.2119-2124

[4] I. Dobson, H. D. Chiang, J. S. Thorp, and L. F. Ahmed, "A Model of Voltage Collapse in Electric Power Systems", *IEEE Proc. of the Conference on Decision and Control*, Austin, Texas, 1988, pp. 2104-2109

[5] V. Ajjarapu and B. Lee, "Bifurcation Theory and Its Application to Nonlinear Dynamical Phenomena in an Electrical Power System", *IEEE Trans. on Power Systems*, Vol.7, No.1, February 1992., pp. 424-431

[6] Venkatasubramanian, V.Schattler, H., and Zaborszky, J., "Global Voltage Dynamics: Study of a Generator with Voltage Control, Transmission and matched MW Load", *Proceedings of the 29th IEEE Conference on Decision and Control*, 1990, pp.3045-3056

[7] Ali H. Nayfeh, Ahmad M. Harb, and Char-ming Chin, "Chaos and Instability in a Power System: Primary Resonant Case", *ISCAS '95., 1995 IEEE International Symposium on Circuits and Systems*, 1995, pp.283-286

[8] Kunder, P., "Power System Stability and Control", *Electric Power Research Institute, McGraw-Hill, Inc.* New York

[9] Ali H. Nayfeh and Balakumar Balachandran, "Applied Nonlinear Dynamics-Analytical, Computational, and Experimental Methods", *Wiley Series in Nonlinear Science*, 1995

[10] Ali H. Nayfeh, "Introduction to Perturbation Techniques", *A Wiley-Interscience Publication*, 1981

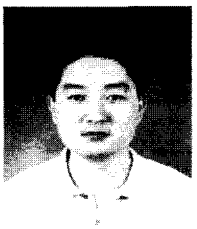

Sang-Ho Lee
He received the Ph.D. in Electrical Eng. from Seoul Nat'l University. His research interests are power systems operation and planning.

Jong-Keun Park
He received the Ph.D. in Electrical Eng. from the University of Tokyo. His research interests are electricity markets and power systems.